

Spray-spinning: a novel method for making alginate/chitosan fibrous scaffold

Jian-Zheng Wang · Xiao-Bo Huang · Jing Xiao ·
Nan Li · Wei-Ting Yu · Wei Wang · Wei-Yang Xie ·
Xiao-Jun Ma · Ying-Li Teng

Received: 25 June 2009 / Accepted: 26 August 2009 / Published online: 16 September 2009
© Springer Science+Business Media, LLC 2009

Abstract The subject of our investigations was the process of obtaining alginate/chitosan polyelectrolyte complex (PEC) fibers. In this study, a novel method named “spray-spinning” was developed for the making of these hybrid fibers. In spray-spinning, a chitosan solution was sprayed into a flowing sodium alginate solution and sheared into streamlines. The elongated streamlines subsequently transformed into alginate/chitosan PEC fibers. Average diameter of the fibers increased with the increasing of chitosan concentration used in spinning. The fibers showed a high water-absorbability of about 45 folds of water to their dry weight and retained their integrity after incubation in Minimum Essential Medium (MEM) for up to 30 days. In vitro co-culture experiments indicated that the fibers could support the three-dimensional growth of HepG2 cells and did not display any cyto-toxicity. Moreover, in vivo implanting experiments indicated that the connective tissue cells infiltrated into the implanted fibrous scaffolds in

3 weeks after surgery. These results demonstrated the potential applications of the as-spun fibers in regenerative medicine and tissue engineering.

1 Introduction

1.1 Three-dimensional (3D) scaffold and fiber-making

Tissue engineering and regenerative medicine aim at the development of biological substitutes restoring, maintaining or improving tissue function [1]. Efforts in this have been directed to produce biocompatible 3D scaffolds that mimic the structure and morphology of native porous extracellular matrix (ECM). The function of these scaffolds is to physically support cells and to provide conditions for cell adhesion and growth. Appropriate material topography, cyto-compatibility, porosity, pore size, permeability, surface properties and mechanical stability have been defined as being critical requirements for the scaffolds [1–3]. According to topographical and architectural characters, the porous 3D scaffolds in biomedical field can be meanly divided into two categories: alveoloid and fibroid. In alveoloid scaffolds, the skeletal structure is integrated into an alveolate framework [4, 5]; in contrast, the skeletal structure in fibroid scaffolds is composed of un-adhering fibers [6, 7]. Fibrous meshes in fibroid scaffold possessing high porosity, high permeability, high interconnectivity of the pores and highly specific surface area may closely mimic the surface structure and morphology of native porous ECM. In addition, the alignment of macromolecular orientation along the fiber direction during the process of fiber-making may greatly increase the modulus of the fibers [8]. Different techniques, such as wet spinning [6, 7], self-assembly [9], in situ fibrillation [10], phase separation

J.-Z. Wang · X.-B. Huang · J. Xiao · N. Li · W.-T. Yu ·
W. Wang · W.-Y. Xie · X.-J. Ma (✉)
Laboratory of Biomedical Material Engineering, Dalian Institute
of Chemical Physics, Chinese Academy of Sciences,
457 Zhongshan Road, 116023 Dalian,
People's Republic of China
e-mail: maxj@dicp.ac.cn

J.-Z. Wang
e-mail: wangjz@dicp.ac.cn

J.-Z. Wang · X.-B. Huang · J. Xiao · N. Li
Graduate School of the Chinese Academy of Sciences,
Chinese Academy of Sciences, 100039 Beijing,
People's Republic of China

Y.-L. Teng
School of Materials Science and Engineering, Dalian Jiaotong
University, 116028 Dalian, People's Republic of China

[11], electrospinning [12] and hydro-spinning [13] have been applied to fabricate these fibers.

1.2 Chitosan and alginate for scaffold-making

The ideal scaffold materials should be nontoxic and biocompatible under physiological conditions after being implanted in human body, and should be completely degraded and resorbed when the tissue is fully regenerated [14]. Chitosan, a de-*N*-acetylated analog of chitin consisting of linear β -1,4-linked GlcN and GlcNAc units [15], has been explored as a suitable functional material for biomedical utilization due to its biodegradability, biocompatibility, and nontoxicity [16]. Apart from chitosan, alginate, a family of linear binary copolymers of (1–4) glycosidically linked residues of α -L-guluronic acid (G) and β -D-mannuronic acid (M) [17], has also been studied extensively owing to its unique biocompatibility in tissue engineering [6, 18–20]. The alginate/chitosan polyelectrolyte complex (PEC) has combined properties of the two individual components, such as more stable to pH change for shape-keeping than alginate or chitosan alone in aqueous medium [21, 22]. Therefore, alginate/chitosan hybrid PEC is also widely used for scaffold-making in biomedical and bioengineering fields [23–25].

1.3 Chitosan and alginate for fibrous scaffold-making

Alginate or chitosan fibers have been produced by electrospinning [18, 26–32] and wet spinning [6, 7, 33–42], respectively. Nevertheless, the electrospun fibers containing alginate or chitosan were actually achieved by blending with synthetic polymer or co-solvent, such as poly(ethylene oxide) (PEO) [18, 26, 27, 31, 32], poly(vinyl alcohol) (PVA) [28, 32], glycerol [29] and trifluoroacetic acid (TFA) [30], etc., for viscosity reasons. Similarly, the wet-spun fibers containing alginate or chitosan were actually achieved by coagulating with cross-linking agent or non-solvent, such as epichlorohydrin (ECH) [34, 40], NaOH [34], CaCl₂ [41] and Methanol [42], etc., for shape-stability reasons. As to alginate/chitosan hybrid fibers, electrospinning of them directly from alginate/chitosan blend solution is difficult, since a direct mixing of the two polymer solutions would readily coagulate and form gels due to the opposite charges between alginate and chitosan. However, alginate/chitosan PEC fibers have been produced by wet spinning [6, 7, 33, 41–43]. Even though, the chitosan content in the fibers is always lower than 15% w/w, since the wet spinning method of making these fibers is based on the principle of coating procedure via ionic interactions. Fan et al. [44] produced the alginate/chitosan fibers by mixing the two solutions before coagulating procedure of the wet spinning. Nevertheless, no further

details described in their article about the uniformity of the two components in the blended mixture.

1.4 Our work in this paper

In previous study [13], we established a method of “hydro-spinning” to make alginate/chitosan PEC hybrid fibers without the assistance of synthetic co-solvent, cross-linking agent or solvent other than thin concentrations of acetic acid and sodium acetate in pure water. In this study, we developed a modified hydro-spinning method, which we named “spray-spinning”, to make these micro-fibers. Instead of injecting a chitosan solution into a flowing sodium alginate solution in our previous “hydro-spinning”, the operation in present “spray-spinning” was simplified to spray a chitosan solution into a flowing sodium alginate solution to make fibers (Fig. 1a). Scanning electron microscope (SEM), Fourier transform infrared spectroscope (FTIR) and optical microscope were employed to characterize the morphology, size and composition of alginate/chitosan spray-spun products. Stability in Minimum Essential Medium (MEM) and water-absorbability of the fibers were also detected. In addition, both in vitro co-culture and in vivo implanting experiments were employed to determine the biocompatibility of these fibers.

2 Materials and methods

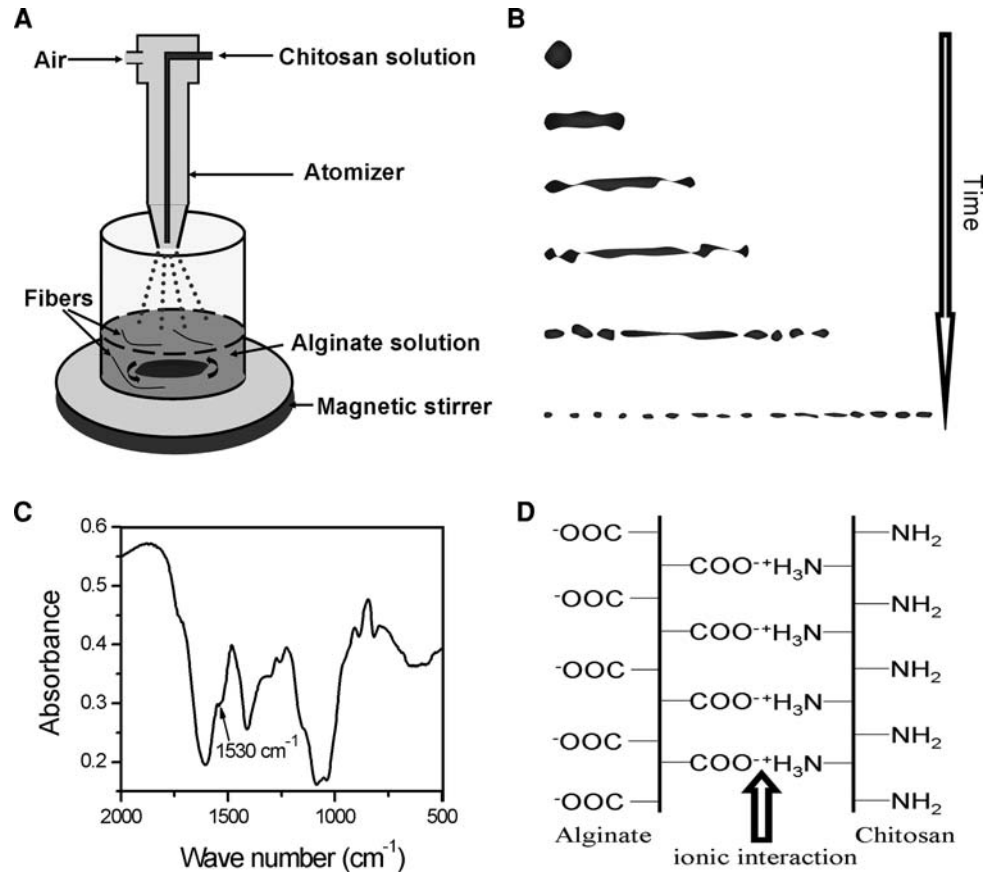
2.1 Materials

Chitosan stock solution (10.0 g/l) was prepared by dissolving chitosan (230 kDa, 98% deacetylation, Yuhuan Ocean Biochemical Co., Ltd., Zhejiang, China) in a solvent of 0.2 M CH₃COOH/0.1 M CH₃COONa and filtered through a 0.2 μ m millipore filter. The working solutions of chitosan (0.500, 0.333 and 0.250 g/l) were prepared by diluting the chitosan stock solution with water, respectively. To prepare alginate solution (1×10^{-2} g/ml), sodium alginate (595 kDa, Jinyan Bio-Tech Development Corporation, Shandong, China) with L-guluronic acid (G)/D-mannuronic acid (M) residue ratio of 0.5 was dissolved into stirring water and then filtered with a 0.2 μ m millipore filter. HepG2 (Human hepatocellular liver carcinoma cell line) was a gift from Professor Kong Li (Dalian Medical University, Dalian, China).

2.2 Spray-spinning alginate/chitosan fibers

Figure 1a shows the schematic equipment of “spray-spinning”. At room temperature ($22.5 \pm 0.5^\circ\text{C}$), a

Fig. 1 **a** Scheme of alginate/chitosan spray-spinning apparatus. Chitosan solution was sprayed into the viscous alginate solution being rotated by a magnetic stirrer. **b** Three-dimensional simulation of droplet breakup in simple shear flow, view along the velocity gradient. A droplet or elongated streamline breaks up to pieces when the velocity gradient reaches a high value. **c** FTIR spectra of the pH neutralized alginate/chitosan spray-spun product. **d** Potential ionic interaction between sodium alginate and chitosan



spray-drying equipment (Shandong Tianli Drying Equipment Co. Ltd.) was employed to spray chitosan solution (100 ml) into a beaker (Φ105 mm) containing alginate solution (300 ml) which was being stirred on a magnetic stirrer. The length of the stir bar was 4.0 cm and the rotate speed was 700 rpm. The distance between sprinkler and alginate solution surface was 10 cm. The liquid pump flux was 900 ml/h and the air flux was 15 l/min.

After fabrication, the spray-spun product was centrifuged and washed with neutral pH water for 3 times (centrifuged after each time). Aligned fibers were collected by sticking a thin stainless steel needle into the rotating water in an additional 4th washing procedure as reported [13]. Samples obtained above were vacuum freezing-dried with a FD-1 vacuum freeze drier (Boyikang laboratory apparatus co., Ltd., Beijing, China).

2.3 Fourier transform-infrared spectroscopy (FTIR)

Sample was pulverized with KBr and pressed into pellet. Infrared spectra were obtained at a resolution of 2 cm⁻¹ on a Bruker Vector 22 fourier transform infrared spectrophotometer (Bruker Optics, Billerica, MA).

2.4 Water absorbability

Water absorbability was measured by a method as previously reported [13]. Briefly, dried sample of weight *W* was immersed in a graduated cylinder containing a known weight (*w*₁) of water. After removing the air from the cylinder, the water-impregnated sample was also removed. The remaining weight of water in the cylinder (*w*₂) was recorded. Water absorbing rate (*A*) was then calculated from the formula:

$$A = \frac{w_1 - w_2}{W} \tag{1}$$

2.5 Elementary analysis

Element compositions (N, C and H) of sample were determined by an elemental vario EL-III Element Analyzer (Analysensysteme GmbH, Germany) according to the instruction and operation manual.

2.6 Scaffold stability test

Fibers were immersed in MEM at 5% CO₂ with humidity to evaluate the stability of scaffold in cell culture system. After 30 days of saturation at 37°C, fibers were rinsed in

PBS and dehydrated in a series of ethanol solutions. Then, the fibers were vacuum freezing-dried.

2.7 In vitro three-dimensional co-culture

According to normal procedure, HepG2 cells were cultured in a complete MEM. As reaching about 90% confluence, the HepG2 cells were removed by trypsin-EDTA and seeded onto the spray-spun fibrous scaffolds at a density of 0.5×10^6 cells/cm². Under dynamic conditions in MEM at 37°C and 5% CO₂, the cell-seeded scaffolds were cultured for 1 week with daily medium changes.

2.8 In vivo rat's thigh implanting test

Bilateral thigh areas of the anesthetized Sprague–Dawley (SD) rats (280–330 g, 7 weeks old) were disinfected and incised to expose leg muscles (Fig. 6d). Certain amounts of spray-spun fibers (about 50 mg for one incision) were implanted into the muscles. Then, the skin incisions were sutured and the animals were administered with a daily intramuscular injection of Benzylpenicillin (10,000 U/day). Three weeks after surgery, the implants were harvested and subjected to paraffin section and HE staining operation.

2.9 Hematoxylin and eosin stain (H&E)

The wet un-lyophilized fibers were stained with hematoxylin and eosin for 20 min. After briefly rinsed with water, the stained fibers were observed with a Nikon Eclipse TE2000 Inverted Research Microscope (Nikon Corporation, Japan) and optical images were taken. For the samples of cell co-cultured scaffold and implanting specimen, paraffin section and HE-staining operations were carried out. Briefly, the samples were fixed in 4% formaldehyde and paraffin-embedded. Sections were cut in 5 μm thicknesses and de-paraffinized. After staining with hematoxylin and eosin, the samples were evaluated with a Nikon Eclipse TE2000 Inverted Research Microscope.

2.10 Confocal laser scanning microscopy (CLSM)

Live/dead viability assay was performed to evaluate the cell viability on the fibrous scaffold. Briefly, cell co-cultured scaffold was incubated with EthD-1 and calcein-AM solution at room temperature for 30 min in the dark, followed by a PBS wash. Then, the preparations were imaged under a Leica TCS SP2 laser scanning confocal microscopy (Leica microsystem Inc., Bannockburn, IL).

2.11 Scanning electron microscopy (SEM)

In vitro co-cultured fibers were rinsed in PBS and fixed in 2.5% glutaraldehyde. Then, the samples were dehydrated in a series of ethanol solutions and vacuum freezing-dried. The unseeded spray-spun samples were directly cut from the WD products. Samples obtained above were sputter-coated with evaporated gold and imaged under a JSM-5600 LV scanning electron microscope (Nippon Denki Co., Ltd., Japan).

2.12 Fiber size measurement

In HE-stained and SEM images of spray-spun fibers, one hundred distinct points were measured for each sample using software ImageJ. Average diameter was determined and presented as mean ± standard deviation.

2.13 Statistical analysis

Statistical comparisons were performed using a one-way analysis of variance (ANOVA); differences at $P \leq 0.05$ were considered statistically significant.

3 Results and discussion

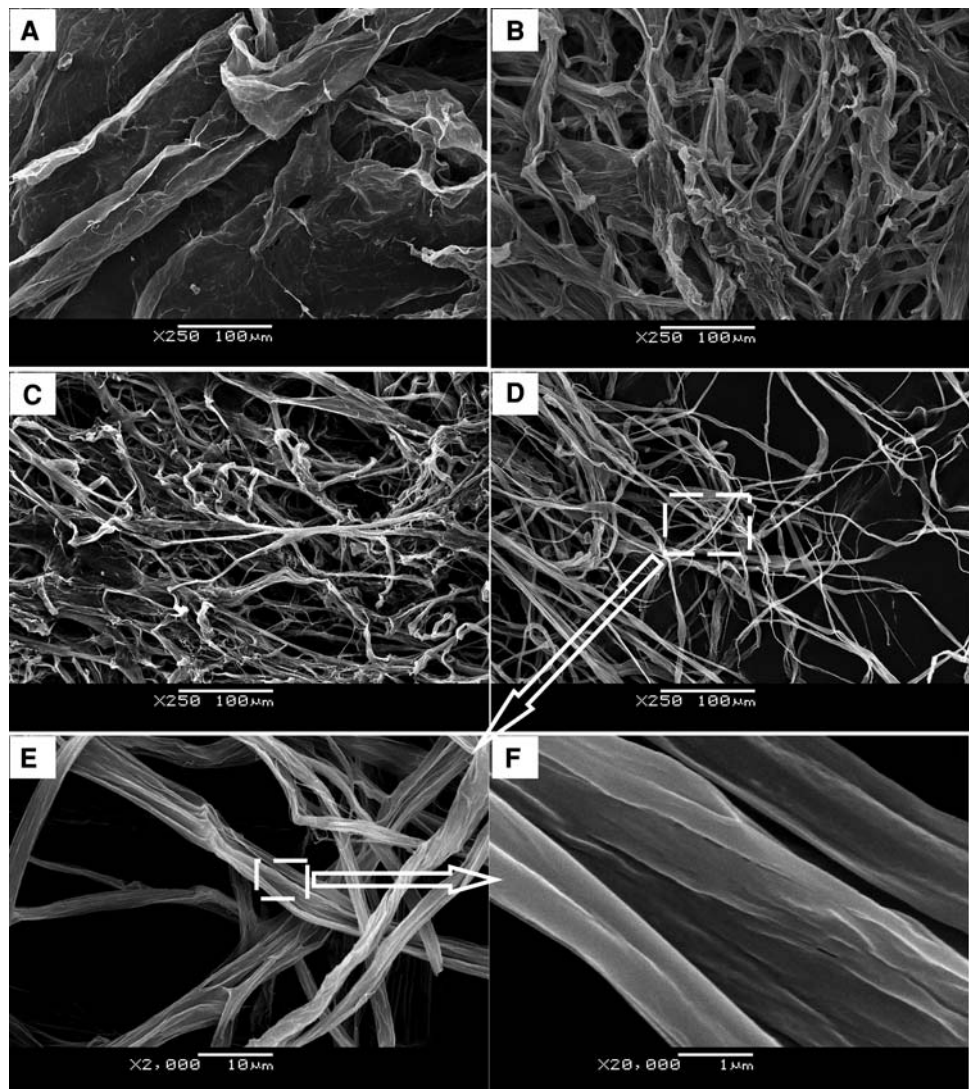
3.1 Electrovalent bond

FTIR were employed to determine the interaction between alginate and chitosan in the spray-spun products. Just as hydro-spun products [13], the spectra of pH neutralized alginate/chitosan spray-spun products also displayed a deforming peak at 1,531 cm⁻¹ which was attributed to the protonated amine of chitosan (Fig. 1c), indicating that alginate combined chitosan with an electrovalent bond by the interactions between the free protonated amino groups (–NH₃⁺) of chitosan and the carboxylate groups (–COO⁻) of alginate (Fig. 1d). Namely, alginate/chitosan PEC formed during the process of spray-spinning. The presence of this PEC might provide the basis for the fiber stability in MEM which will be referred to later.

3.2 Morphology and fiber size

In this work, a series of chitosan solutions (10.0, 0.500, 0.333 and 0.250 g/l) were used for spray-spinning and the spun products was marked as CA_{10.0}, CA_{0.500}, CA_{0.333} and CA_{0.250}, respectively. Water freezing-dried (WD) products spun at chitosan concentration of 10.0 g/l (WD CA_{10.0}) presented as laminar morphology under SEM observation (Fig. 2a); in contrast, the WD products spun at lower chitosan concentrations of 0.500, 0.333 and 0.250 g/l

Fig. 2 SEM images of spray-spun products: **a** products spun at chitosan concentration of 10.0 g/l (WD CA_{10.0}); **b** products spun at chitosan concentration of 0.500 g/l (WD CA_{0.500}); **c** products spun at chitosan concentration of 0.333 g/l (WD CA_{0.333}); **d–f** products spun at chitosan concentration of 0.250 g/l (WD CA_{0.250}). **e** and **f** are enlarged partial views of **d**



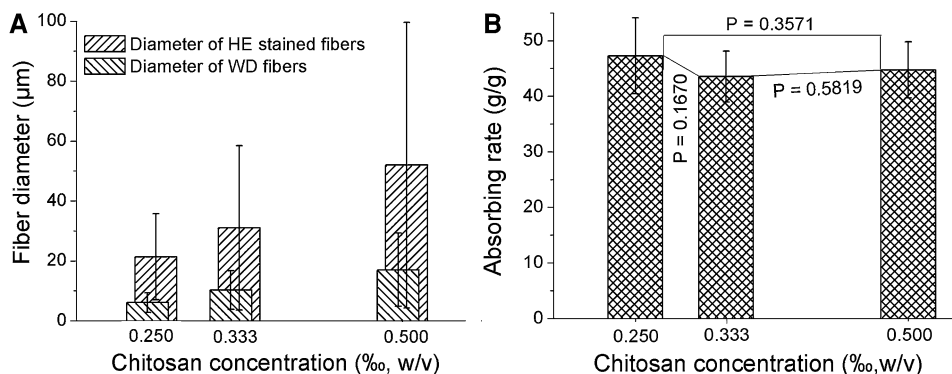
presented as slender fibers (Fig. 7a). Some irregular fragments were observed in these samples. These fragments were speculated to be produced by the oscillation of alginate flow in spinning process. By going through the additional needle-collecting procedure [13], the irregular fragments could be effectively removed (Fig. 2b–f). Macroscopically, the vacuum freezing-dried fibers presented as a cotton-like construct (Fig. 6c).

Needle-collected products spun at chitosan solution of 0.500, 0.333 and 0.250 g/l appeared as pink ribbons after HE-staining (Fig. 7b). On the assumption that the width of HE-stained fibers in the optical images was the diameter of wet fibers, we observed that the fiber diameter decreased with the decreasing of chitosan concentration used in spinning: diameter of HE-stained CA_{0.500}, HE-stained CA_{0.333} and HE-stained CA_{0.250} was 51.94 ± 47.65 , 31.04 ± 27.44 and 21.39 ± 14.40 μm , respectively (Fig. 3a). These results are consistent with the measurement of WD fibers in SEM images: diameter of WD

CA_{0.500}, WD CA_{0.333} and WD CA_{0.250} was 17.01 ± 12.23 , 10.26 ± 6.51 and 6.06 ± 3.33 μm , respectively (Fig. 3a).

For the rationale of spray-spinning, it could be retrospectively to the droplet breakup problem which was mentioned in many articles [13, 45–49]. A droplet or elongated streamline breaks up to pieces when the velocity gradient reaches a high value (Fig. 1b) [45, 49]. During the process of spray-spinning, the friction at the interface between the continuously mobile alginate solution and the sprayed chitosan droplet results in the droplet elongation. The elongated droplet streamline could change into PEC fiber before it breaks up into pieces (Fig. 4d). Reports indicated that the fragility of a fluidic streamline in viscous liquid is strongly dependent on the viscosity ratio λ , where $\lambda = \mu_d/\mu_m$, μ_d and μ_m denote the viscosity of elongated streamline and matrix, respectively [46, 49]. Therefore, the droplet elongation process in spray-spinning might be largely affected by the viscosity ratio of the viscosity of chitosan solution to the viscosity of alginate solution. It is a

Fig. 3 **a** HE stained fiber diameters measured in optical images and water freezing-dried (WD) fiber diameters measured in SEM images. **b** Water absorbing rates (g/g) of WD fibers



known fact that viscosity of a polymer solution is largely determined by the concentration and molecular weight of its polymeric solute. Although chitosan is unstable in acetic acid solution, the relative viscosity and molecular weight of chitosan decrease very slowly with increasing storage time in the low concentration of acetic acid solutions [50]. Nevertheless, acetic acid may have direct effects on the chitosan solution's viscosity as the solute chitosan does [51, 52]. Since working solutions in our spinning were diluted from chitosan stock solution by pure water (see Sect. 2), changing the chitosan concentration simultaneously changed the acetic acid concentration. Both of these two concentration alterations might influence the

viscosity of chitosan solution, consequently influencing the viscosity ratio λ between alginate and chitosan solutions; as a result, the spray-spun product's properties, such as the fiber diameter, would change accordingly. The experimental results shown in Fig. 3a verified the aforementioned inference.

Interestingly, although the liquid pump flux in spray-spinning (900 ml/h) was much larger than that in hydro-spinning (118.8 ml/h) [13], the spray-spun fibers did not show larger fiber diameter that much than hydro-spun fibers at the same chitosan concentration (in SEM images, the upmost diameters at chitosan concentration of 0.333 g/l were both no more than several tens of micrometers in the two methods). This might be attributed to the much more contact area in spray-spinning than that in hydro-spinning: in hydro-spinning, only one fiber streamline was forming in the alginate solution from one needle tip at a time; while in spray-spinning, numerous fiber streamlines were forming on the alginate solution's surface from droplets sprayed by one sprinkler at the same time (Fig. 1a). This reminds us that, comparing with hydro-spinning, the operation of spray-spinning is not only simpler, but might be more efficient.

It is worth mentioning that flow fields used in processing of polymers can be mainly divided into two categories: [13, 53] shear flow (Fig. 4a) and extensional flow (Fig. 4b) (elongational flow). Just as in hydro-spinning [13], the flow field in spray-spinning belongs to a kind of shear flow (Fig. 4d). This is the essential difference between the spray-spinning and the traditional in situ fibrillation [10, 54]: for the later, its flow field belongs to a kind of extensional flow (Fig. 4c).

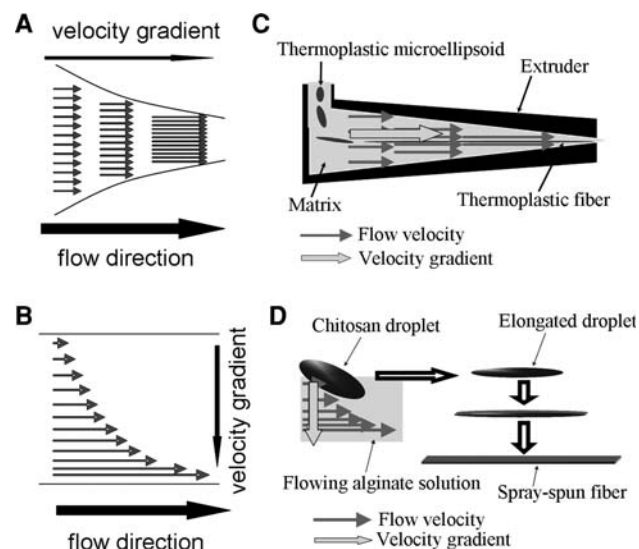


Fig. 4 Flow field and spinning. **a** Extensional flow: the velocity gradient is in parallel with the flow direction. **b** Shear flow: the velocity gradient (shear rate) is perpendicular to the flow direction. **c** Schematic diagram of flow field in in situ fibrillation. Immiscible matrix and thermoplastics are blended and melted in the extruder. The melted thermoplastics droplets are drawn into streamlines by fibrillation process through a caliber-diminishing pipe (and then solidified into fibers by annealing). **d** Flow field in spray-spinning: spinning solution (chitosan solution) is sprayed into and sheared by the flowing alginate solution. Then, the elongated droplet streamline is solidified into an alginate/chitosan PEC fiber (**a** and **b** are reproduced from Ref. [13])

3.3 Water absorbability

For water absorbability is one parameter to evaluate porosity of biomaterial scaffold, we measured the water absorbing rates of WD spray-spun fibers. As shown in Fig. 3b, water absorbing rate of WD CA_{0.500}, WD CA_{0.333} and WD CA_{0.250} was 44.72 ± 5.04, 43.52 ± 4.58 and 47.26 ± 6.83 g/g, respectively. There was no significant

difference between these fibers ($P > 0.05$, Fig. 3b). Assuming density of water is 1.00 g/ml, the average porosity of these fibers was approximately 45 ml/g. The high water absorbability of these fibers might be attributed to the large porosity of their assembly (Fig. 2b–d). In addition, it could be found from high resolution that the surface of these fibers is full of wrinkles (Fig. 2e–f), indicating the fibers had large specific surface area which might also help to increase their water absorbability. The large porosity and specific surface area of these fibers might be helpful for the cell adhesion and infiltration, and the nutriment penetration in cell culture.

3.4 Element compositions and chitosan content

Elementary analysis results of spray-spun products are shown in Table 1. The ratio of nitrogen to carbon (N/C) of CA_{0.500}, CA_{0.333} and CA_{0.250} was 0.096 ± 0.001 , 0.089 ± 0.003 and 0.089 ± 0.001 , respectively. Previously [13], we reported that the ratio N/C of pure chitosan (230 kDa) and pure alginate (595 kDa) was 0.194 ± 0.003 and 0.000 ± 0.000 , respectively. Assuming the mean N/C value of pure 230 kDa chitosan sample (which was 0.194) is the real ratio N/C of chitosan (γ_0), percentage content of chitosan (H) in a sample was calculated from the following formula:

$$H = \frac{\gamma}{\gamma_0} \times 100\% \tag{2}$$

where γ is the ratio N/C in a sample and $\gamma_0 = 0.194$ [13]. Then, the chitosan content of CA_{0.500}, CA_{0.333} and CA_{0.250} was 49.5 ± 0.6 , 45.7 ± 1.6 and $45.8 \pm 0.4\%$ w/w, respectively (see Table 1). Comparing with wet spinning and hydro-spinning, the chitosan content in spray-spun fibers is slightly lower than that in hydro-spun fibers (in which the chitosan content is about 45–55% [13]), but is much higher than that in wet-spun fibers (in which the chitosan content is about 1–25% [7]).

3.5 Fiber stability

To evaluate stability of the spray-spun fibrous scaffold in cell culture, blend fibers of WD CA_{0.500}, WD CA_{0.333} and

WD CA_{0.200} were immersed in MEM medium at 37°C and 5% CO₂ with humidity. Result indicated that the fibers retained their integrity in appearance after 30 days of incubation in MEM (Fig. 5a–c). This indicates that, comparing with alginate and chitosan which are soluble in MEM, the spray-spun fibers were stable and might undergo saturation in cell culture system up to 1 month. This might be attributed to the presence of alginate/chitosan PEC in the fibers.

3.6 Bio-compatibility

Excellent bio-compatibility is a prerequisite for cell scaffold in the fabrication of tissue substitutes. Therefore, cyto-compatibility of the alginate/chitosan spray-spun fibers was evaluated by co-culturing with HepG2 cells in vitro. Under optical observation, it was found that HepG2 cell clusters formed 5 days after cell seeding, indicating three-dimensional growth of the co-cultured cells on the scaffold (Fig. 6a). Live/dead assay was applied to detect the cell viability and CLSM images indicated that most of these cells were stained into green fluorescence (Fig. 6b), showing they were alive 5 days after cell seeding. The cell activity was also confirmed by the H&E stain and SEM observation. In H&E stain images, the acidophilic alginate/chitosan scaffolds were stained with eosin into pink ribbons and the cells were stained with hematoxylin into purple cluster-beads (Fig. 7c). In SEM images, the cells assembled into three-dimensional mass (Fig. 5d, g). In addition, the conglobate cells of tri-dimensionally growing cell-blocks possessed abundant ECM nano-fibers on the cellular surface (Fig. 5d–i), demonstrating good activity of these cells on the scaffold.

In vivo biocompatibility of the fibers was also evaluated by implanting the fibers into the rat leg muscle (Fig. 6c, d). Typical histological picture of the implanted scaffold specimens is presented in Fig. 7d. From the image, we observed that large numbers of connective tissue cells infiltrated into the implanted fibrous scaffold 3 weeks after surgery, showing good biocompatibility of the scaffold in vivo.

Table 1 Element analysis data of spray-spun fibers (data showed as mean \pm SD, $n = 4$)

Sample	N (%)	C (%)	H (%)	N/C	CC ^a
CA _{0.500}	3.39 \pm 0.10	35.2 \pm 0.7	6.18 \pm 0.18	0.096 \pm 0.001	49.5 \pm 0.6
CA _{0.333} ^b	3.12 \pm 0.10	35.2 \pm 0.1	6.07 \pm 0.05	0.089 \pm 0.003	45.7 \pm 1.6
CA _{0.250} ^b	3.08 \pm 0.03	34.7 \pm 0.1	6.16 \pm 0.13	0.089 \pm 0.001	45.8 \pm 0.4

^a CC (chitosan content, %) = $100 \times (N/C)/0.194$

^b There was no significant difference between the data of CA_{0.333} and CA_{0.250} ($P > 0.05$)

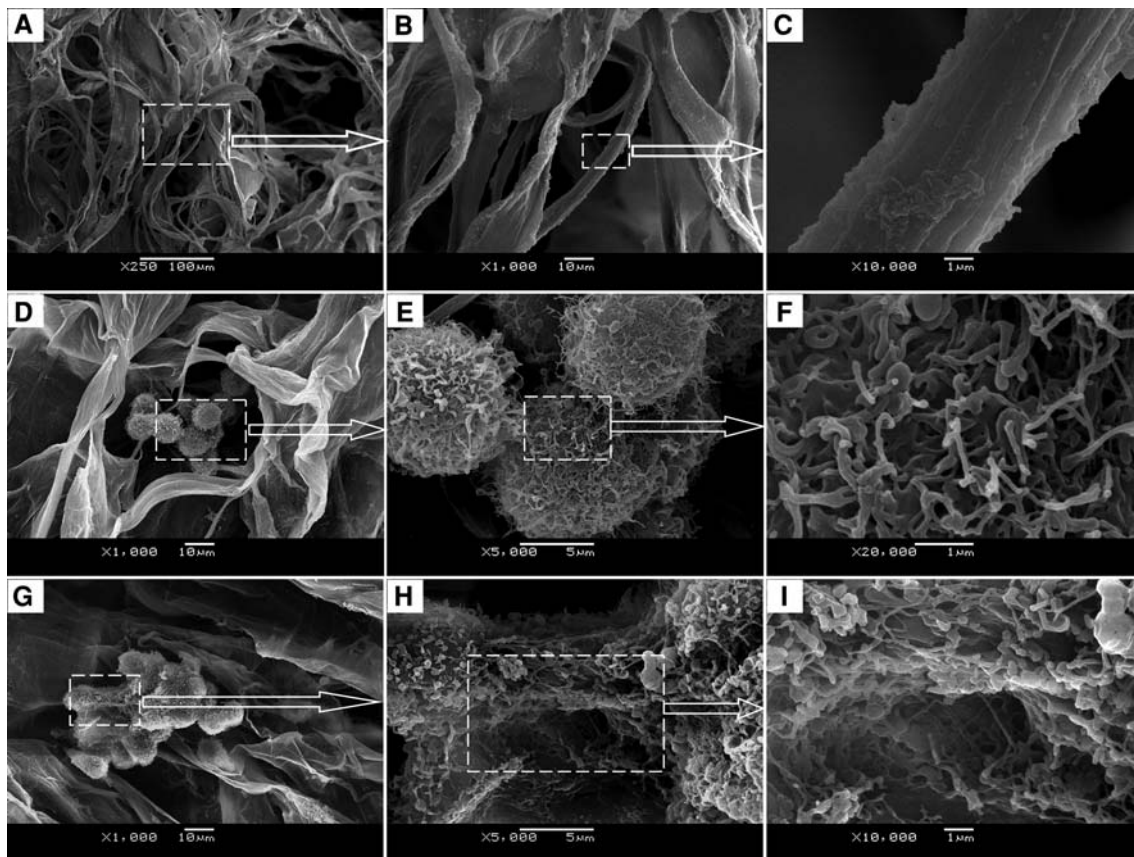


Fig. 5 a–c SEM images of fibers saturated in MEM up to 30 days: b and c are enlarged partial views of a. d–i SEM images of cellular clusters on fibrous scaffold 5 days after seeding: e and f are enlarged partial views of d; h and i are enlarged partial views of g

Fig. 6 a Optical image of cell clusters (white arrows) on the fibrous scaffold 5 days after seeding. b CLSM fluorescence image of cell clusters on fibrous scaffold 5 days after cell seeding (live/dead viability assay). c Water freezing-died fibers for implanting (stereoscopic image). d Implanting region (white arrow) of the fibers

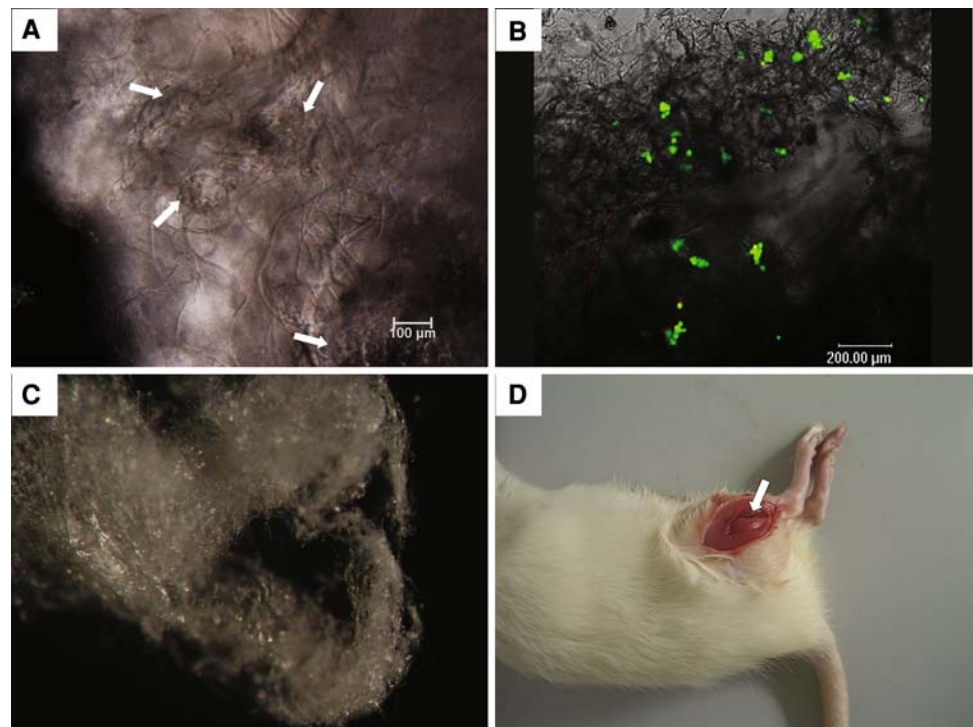
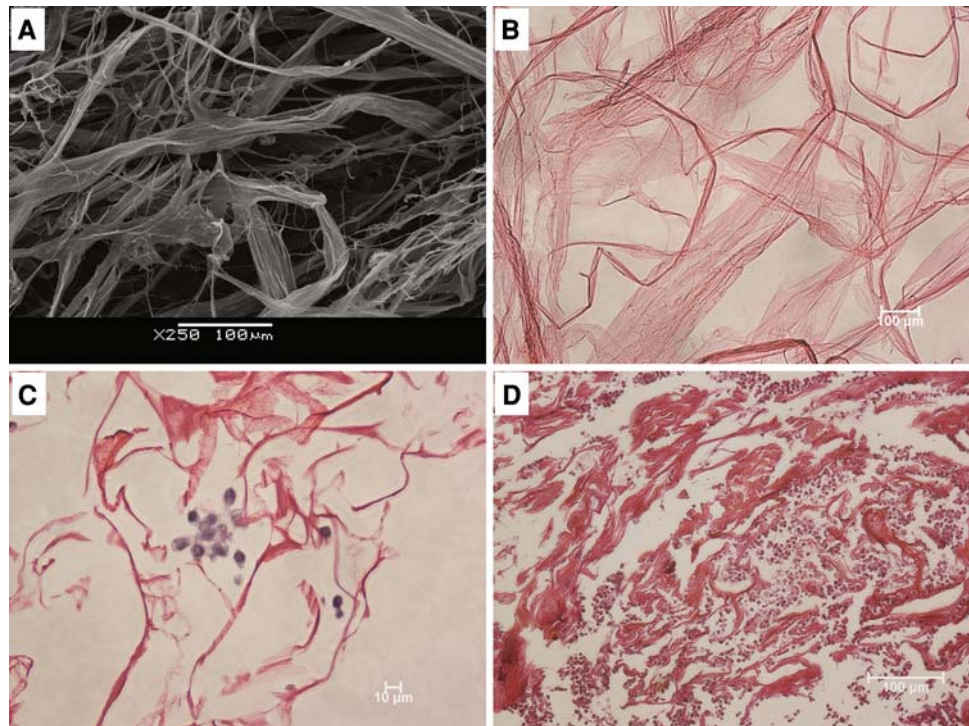


Fig. 7 **a** Fragment-containing sample without going through the additional needle collecting-procedure; **b** HE-stained wet fibers; **c** HE stain images of cell culture construct 5 days after seeding; **d** HE histological picture of the implanted scaffold specimen 3 weeks after surgery: large numbers of connective tissue cells infiltrated into the implanted fibrous scaffold



4 Conclusions

This work described a new method of “spray-spinning”, which was a modified technique from previously reported “hydro-spinning”, for the fabrication of alginate/chitosan PEC strap-like fibers. A chitosan solution was sprayed into a flowing sodium alginate solution and sheared into streamlines. The elongated streamlines subsequently transformed into alginate/chitosan PEC fibers. Investigations indicated that the size of the spray-spun fibers was affected by the concentration of chitosan solution used in spinning. The chitosan content of the fibers was about 45–50% w/w. Water absorbing rate of the fibers was approximately 45 folds of water to their dry weight, showing that these fibers had a large porosity. Besides, the spray-spun fibers were stable in MEM and retained their integrity after saturation in the medium for 30 days. In vitro experiments demonstrated that HepG2 cells presented a three-dimensional growth on the spray-spun fibrous scaffolds and in vivo experiments indicated that the rat leg connective tissue cells could infiltrate into the scaffold, suggesting the products have a good biocompatibility and might be useful for various applications in regeneration medicine and tissue engineering.

Acknowledgements This study was sponsored by National Basic Research Program of China (under grant number: 2005CB522702), National Natural Science Foundation of China (under grant number: 20736006), Hi-Tech Research and Development (863) Program of China (under grant number: 2006AA02A140), and National Key Sci-Tech Special Project of China (under grant number: 2008ZX10002-019).

References

- Martins A, Araujo JV, Reis RL, Neves NM. Electrospun nano-structured scaffolds for tissue engineering applications. *Nano-medicine*. 2007;2:929–42.
- Karageorgiou V, Kaplan D. Porosity of 3D biomaterial scaffolds and osteogenesis. *Biomaterials*. 2005;26:5474–91.
- Yang SF, Leong KF, Du ZH, Chua CK. The design of scaffolds for use in tissue engineering. Part 1. Traditional factors. *Tissue Eng*. 2001;7:679–89.
- Li ZS, Zhang MQ. Chitosan-alginate as scaffolding material for cartilage tissue engineering. *J Biomed Mater Res A*. 2005;75:485–93.
- Seo SJ, Kim IY, Choi YJ, Akaike T, Cho CS. Enhanced liver functions of hepatocytes cocultured with NIH 3T3 in the alginate/galactosylated chitosan scaffold. *Biomaterials*. 2006;27:1487–95.
- Shao X, Hunter CJ. Developing an alginate/chitosan hybrid fiber scaffold for annulus fibrosus cells. *J Biomed Mater Res A*. 2007;82:701–10.
- Steplewski W, Wawro D, Niekraszewicz A, Ciechanska D. Research into the process of manufacturing alginate-chitosan fibres. *Fibres Text East Eur*. 2006;14:25–31.
- Lu JW, Zhang ZP, Ren XZ, Chen YZ, Yu J, Guo ZX. High-elongation fiber mats by electrospinning of polyoxymethylene. *Macromolecules*. 2008;41:3762–4.
- Harterink JD, Beniash E, Stupp SI. Peptide-amphiphile nanofibers: a versatile scaffold for the preparation of self-assembling materials. *Proc Natl Acad Sci*. 2002;99:5133–8.
- Wang D, Sun G, Chiou BS. A high-throughput, controllable, and environmentally benign fabrication process of thermoplastic nanofibers. *Macromol Mater Eng*. 2007;292:407–14.
- Yang F, Murugan R, Ramakrishna S, Wang X, Ma YX, Wang S. Fabrication of nano-structured porous PLLA scaffold intended for nerve tissue engineering. *Biomaterials*. 2004;25:1891–900.
- Heydarkhan-Hagvall S, Schenke-Layland K, Dhanasopon AP, Rofail F, Smith H, Wu BM, et al. Three-dimensional electrospun

- ECM-based hybrid scaffolds for cardiovascular tissue engineering. *Biomaterials*. 2008;29:2907–14.
13. Wang JZ, Huang XB, Xiao J, Yu WT, Wang W, Xie WY, Zhang Y, Ma XJ. Hydro-spinning: a novel technology for making alginate/chitosan fibrous scaffold. *J Biomed Mater Res A*. doi: 10.1002/jbm.a.32590.
 14. Cheung HY, Lau KT, Lu TP, Hui D. A critical review on polymer-based bio-engineered materials for scaffold development. *Compos Part B*. 2007;38:291–300.
 15. Prashanth KVH, Tharanathan RN. Chitin/chitosan: modifications and their unlimited application potential: an overview. *Trends Food Sci Tech*. 2007;18:117–31.
 16. Muzzarelli RAA. Chitins and chitosans for the repair of wounded skin, nerve, cartilage and bone. *Carbohydr Polym*. 2009;76:167–82.
 17. Augst AD, Kong HJ, Mooney DJ. Alginate hydrogels as biomaterials. *Macromol Biosci*. 2006;6:623–33.
 18. Bhattarai N, Li ZS, Edmondson D, Zhang MQ. Alginate-based nanofibrous scaffolds: structural, mechanical, and biological properties. *Adv Mater*. 2006;18:1463–7.
 19. Dvir-Ginzberg M, Gamlieli-Bonshtein I, Agbaria R, Cohen S. Liver tissue engineering within alginate scaffolds: effects of cell-seeding density on hepatocyte viability, morphology, and function. *Tissue Eng*. 2003;9:757–66.
 20. Dar A, Shachar M, Leor J, Cohen S. Optimization of cardiac cell seeding and distribution in 3D porous alginate scaffolds. *Bio-technol Bioeng*. 2002;80:305–12.
 21. Yan XL, Khor E, Lim LY. PEC films prepared from chitosan-alginate coacervates. *Chem Pharm Bull*. 2000;48:941–6.
 22. Wang LH, Khor E, Lim LY. Chitosan \pm alginate \pm CaCl₂ system for membrane coat application. *J Pharm Sci*. 2001;90:1134–42.
 23. Li ZS, Ramay HR, Hauch KD, Xiao DM, Zhang MQ. Chitosan-alginate hybrid scaffolds for bone tissue engineering. *Biomaterials*. 2005;26:3919–28.
 24. Yang Y, He Q, Duan L, Cui Y, Li J. Assembled alginate/chitosan nanotubes for biological application. *Biomaterials*. 2007;28:3083–90.
 25. Sun ZJ, Lv GJ, Li SY, Yu WT, Wang W, Xie YB, et al. Differential role of microenvironment in microencapsulation for improved cell tolerance to stress. *Appl Microbiol Biotechnol*. 2007;75:1419–27.
 26. Vondran JL, Sun W, Schauer CL. Crosslinked, electrospun chitosan-poly(ethylene oxide) nanofiber mats. *J Appl Polym Sci*. 2008;109:968–75.
 27. Lu JW, Zhu YL, Guo ZX, Hu P, Yu J. Electrospinning of sodium alginate with poly(ethylene oxide). *Polymer*. 2006;47:8026–31.
 28. Zhou YS, Yang DZ, Nie J. Electrospinning of chitosan/poly(vinyl alcohol)/acrylic acid aqueous solutions. *J Appl Polym Sci*. 2006;102:5692–7.
 29. Nie H, He A, Zheng J, Xu S, Li J, Han CC. Effects of chain conformation and entanglement on the electrospinning of pure alginate. *Biomacromolecules*. 2008;9:1362–5.
 30. Ohkawa K, Cha DI, Kim H, Nishida A, Yamamoto H. Electrospinning of chitosan. *Macromol Rapid Comm*. 2004;25:1600–5.
 31. Bhattarai N, Edmondson D, Veiseh O, Matsen FA, Zhang M. Electrospun chitosan-based nanofibers and their cellular compatibility. *Biomaterials*. 2005;26:6176–84.
 32. Safi S, Morshed M, Ravandi SAH, Ghiaci M. Study of electrospinning of sodium alginate, blended solutions of sodium alginate/poly(vinyl alcohol) and sodium alginate/poly(ethylene oxide). *J Appl Polym Sci*. 2007;104:3245–55.
 33. Knill CJ, Kennedy JF, Mistry J, Miraftab M, Smart G, Grocock MR, et al. Alginate fibres modified with unhydrolysed and hydrolysed chitosans for wound dressings. *Carbohydr Polym*. 2004;55:65–76.
 34. Lee SH, Park SY, Choi JH. Fiber formation and physical properties of chitosan fiber crosslinked by epichlorohydrin in a wet spinning system: the effect of the concentration of the cross-linking agent epichlorohydrin. *J Appl Polym Sci*. 2004;92:2054–62.
 35. Su J, Zheng Y, Wu H. Generation of alginate microfibers with a roller-assisted microfluidic system. *Lab Chip*. 2009;9:996–1001.
 36. Yang Q, Dou FD, Liang BR, Shen Q. Investigations of the effects of glyoxal cross-linking on the structure and properties of chitosan fiber. *Carbohydr Polym*. 2005;61:393–8.
 37. Hirano S, Midorikawa T. Novel method for the preparation of *N*-acylchitosan fiber and *N*-acylchitosan-cellulose fiber. *Biomaterials*. 1998;19:293–7.
 38. Tamura H, Tsuruta Y, Itoyama K, Worakitkanchanakul W, Rujiravanit R, Tokura S. Preparation of chitosan filament applying new coagulation system. *Carbohydr Polym*. 2004;56:205–11.
 39. Hirano S, Moriyasu T. Some novel *N*-(carboxyacyl)chitosan filaments. *Carbohydr Polym*. 2004;55:245–8.
 40. Lee SH, Kim Y, Kim Y. Effect of the concentration of sodium acetate (SA) on crosslinking of chitosan fiber by epichlorohydrin (ECH) in a wet spinning system. *Carbohydr Polym*. 2007;70:53–60.
 41. Tamura H, Tsuruta Y, Tokura S. Preparation of chitosan-coated alginate filament. *Mater Sci Eng C*. 2002;20:143–7.
 42. Iwasaki N, Yamane ST, Majima T, Kasahara Y, Minami A, Harada K, et al. Feasibility of polysaccharide hybrid materials for scaffolds in cartilage tissue engineering: evaluation of chondrocyte adhesion to polyion complex fibers prepared from alginate and chitosan. *Biomacromolecules*. 2004;5:828–33.
 43. Watthanaphanit A, Supaphol P, Furuie T, Tokura S, Tamura H, Rujiravanit R. Novel chitosan-spotted alginate fibers from wet-spinning of alginate solutions containing emulsified chitosan-citrate complex and their characterization. *Biomacromolecules*. 2009;10:320–7.
 44. Fan LH, Du YM, Zhang BZ, Yang JH, Cai J, Zhang LN, et al. Preparation and properties of alginate/water-soluble chitin blend fibers. *J Macromol Sci A*. 2005;42:723–32.
 45. Sibillo V, Pasquariello G, Simeone M, Cristini V, Guido S. Drop deformation in microconfined shear flow. *Phys Rev Lett*. 2006;97:054502.
 46. Grace HP. Dispersion phenomena in high viscosity immiscible fluid systems and application of static mixers as dispersion devices in such systems. *Chem Eng Commun*. 1982;14:225–77.
 47. Stone HA. Dynamics of drop deformation and breakup in viscous fluids. *Annu Rev Fluid Mech*. 1994;26:65–102.
 48. Renardy Y. Drop oscillations under simple shear in a highly viscoelastic matrix. *Rheol Acta*. 2008;47:89–96.
 49. Verdier C, Brizard M. Understanding droplet coalescence and its use to estimate interfacial tension. *Rheol Acta*. 2002;41:514–23.
 50. Zoldners J, Kiseleva T, Kaiminsh I. Influence of ascorbic acid on the stability of chitosan solutions. *Carbohydr Polym*. 2005;60:215–8.
 51. Homayoni H, Ravandi SAH, Valizadeh M. Electrospinning of chitosan nanofibers: processing optimization. *Carbohydr Polym*. 2009;77:656–61.
 52. Geng XY, Kwon OH, Jang JH. Electrospinning of chitosan dissolved in concentrated acetic acid solution. *Biomaterials*. 2005;26:5427–32.
 53. Ballman RL. Extensional flow of polystyrene melt. *Rheol Acta*. 1965;4:137–40.
 54. Jiang CH, Zhong GJ, Li ZM. Recyclability of in situ microfibrillar poly(ethylene terephthalate)/high-density polyethylene blends. *Macromol Mater Eng*. 2007;292:362–72.